Proceedings of the 36th European Peptide Symposium
Michal Lebl (Editor)
European Peptide Society, 2022 *https://doi.org/10.17952/36EPS.2022.213*

Synthesis and Analysis of Structure-Activity Relationship of Antimicrobial Peptide Conjugates Incorporating a Plant Defence Elicitor

Gerard Riesco-Llach[1], Pau Caravaca-Fuentes[1,2], Àngel Oliveras[1], Sergio Gil-Caballero[3], Esther Badosa[2], Anna Bonaterra[2], Emilio Montesinos[2], Marta Planas[1], and Lidia Feliu[1]

[1]LIPPSO, Department of Chemistry, University of Girona, Girona, 17003, Spain; [2]Laboratory of Plant Pathology, Institute of Food and Agricultural Technology-CIDSAV-XaRTA, University of Girona, Girona, 17003, Spain; [3]Serveis Tècnics de Recerca (NMR), University of Girona, Parc Científic i Tecnològic, Girona, 17003, Spain

Introduction

According to United Nations, it is expected that at the end of this century the world population will rise to more than 10 thousand million. In this context, agriculture will face major challenges in terms of food production. One of the main threats are plant diseases caused by bacteria and fungi which have a huge impact on crop production involving important economic loses. It is worth noting that there are not many effective methods to tackle some of these diseases, and the antibiotics available are not authorized in Europe. Within this field, antimicrobial peptides have attracted much attention as new agents to control phytopathogens: apart from being more environmentally friendly than traditional pesticides they are less prone to causing the appearance of resistant strains [1].

Different strategies have been described to enhance the biological profile of antimicrobial peptides such as the incorporation of a fatty acid chain to increase the interaction with bacterial membranes or even the combination of two peptides with different biological activity to obtain a new bifunctional sequence [2,3,4].

In our group we have recently reported the synthesis of peptide conjugates incorporating an antimicrobial sequence, derived from the lead peptide **BP100** (KKLFKKILKYL-NH_2), and a plant defense elicitor. These conjugates were screened for their antimicrobial activity against bacterial pathogens, their hemolytic activity, and their effect on plant defense gene expression [5].

Based on the promising biological activity profile exhibited by this collection of peptide conjugates, the aim of this work was to perform a structure-activity relationship analysis. For this purpose, we selected 6 peptide conjugates including highly and poorly active sequences and with a range of hemolysis to relate their biological activity with physicochemical parameters that govern their mechanism of action.

Results and Discussion

Peptide conjugates were designed by combining an antimicrobial peptide (**BP16**, **BP100**, or **BP475**) at the *N*- or *C*- terminus of a reported plant defence elicitor peptide (**flg15**, **BP13** or **Pep13**). Their synthesis was performed on solid phase following a 9-fluorenylmethoxycarbonyl (Fmoc)/*tert*-butyl (*t*Bu) strategy using a ChemMatrix resin as solid support. For the preparation of peptide amides, a Fmoc-Rink amide linker was employed, whereas a PAC linker was used for those containing a carboxylic acid at the *C*-terminus. Peptide elongation was carried out through sequential steps of Fmoc removal with piperidine/DMF and coupling of the protected amino acids with *N*,*N*- diisopropylcarbodiimide (DIC) and ethyl 2-cyano-2-(hydroxyimino)acetate (Oxyma). For the sequences incorporating a fatty acid at the side-chain of a lysine (**BP475**), this residue was incorporated as Fmoc-Lys(ivDde)-OH. The 1-(4,4-dimethyl-2,6-dioxocyclohex-1-ylidine)-3-methylbutyl (ivDde) group was chosen because it is stable to the treatments with piperidine and can be removed with hydrazine, allowing the selective derivatization of this residue. Finally, an acidolytic cleavage afforded the expected peptide conjugates which after purification were obtained in excellent HPLC purities and were characterized by ESI-HRMS (Table 1).

Table 1. Sequences of the peptide conjugates, HPLC retention times (t_R) and purities, and mass spectrometry results.

Peptide conjugate	*Sequence*[a]	*t_R (min)*	*Purity (%)*	*ESI-HRMS*
flg15-BP475	Ac-RINSAKDDAAGLQIA-KKLfKKILKK(COC_3H_7)L-NH_2	6.79	97	1511.4329
BP475-flg15	Ac-KKLfKKILKK(COC_3H_7)L-RINSAKDDAAGLQIA-OH	6.03	>99	1511.9271
Pep13-BP100	VWNQPVRGFKVYE-KKLFKKILKYL-NH_2	6.14	>99	1512.4007
BP100-Pep13	KKLFKKILKYL-VWNQPVRGFKVYE-OH	5.53	>99	1512.8950
BP13-BP16	FKLFKKILKVL-KKLFKKILKKL-NH_2	7.85	>99	1372.4666
BP16-BP13	KKLFKKILKKL-FKLFKKILKVL-NH_2	7.68	>99	1372.4627

[a]*COC_3H_7, butanoyl. Lowercase letters correspond to D-amino acids*

Peptide conjugates were tested *in vitro* against six plant pathogenic bacteria: *Xanthomonas axonopodis* pv. vesicatoria (*Xav*), *Xanthomonas fragariae* (*Xf*), *Xanthomonas arboricola* pv. pruni (*Xap*), *Erwinia amylovora* (*Ea*), *Pseudomonas syringae* pv. syringae (*Pss*) and *Pseudomonas syringae* pv. actinidiae (*Psa*). For all of them, the minimum inhibitory concentration (MIC) was determined (Figure 1A). Peptides incorporating **flg15** or **Pep13** were more active against these phytopathogens than those containing **BP13**. In particular, **flg15-BP475**, **BP475-flg15**, **Pep13-BP100** and **BP100-Pep13** exhibited MIC values <6.2 μM against at least five of the bacteria tested. Moreover, the hemolytic activity of the peptides was assessed by determining hemoglobin release from erythrocytes at 150 μM peptide concentration (Figure 1B). In this case, peptide conjugates derived from **BP13** were the most hemolytic, with hemolysis >85%. In contrast, **BP475-flg15** was not hemolytic and the other conjugates showed hemolysis between 25 and 45%.

These biological results can be related to physicochemical parameters of the peptide conjugates such as the charge, the hydrophobicity, or the secondary structure that they adopt. In this context, we elucidated the structure of six peptide conjugates by NMR in presence of 30% CF_3CD_2OD (TFE-d_3). The secondary structure was predicted by the Chemical Shift Index based on the ^{1}H-, ^{13}C- and ^{15}N-chemical shifts and was confirmed by NOESY and TOCSY correlations [6].

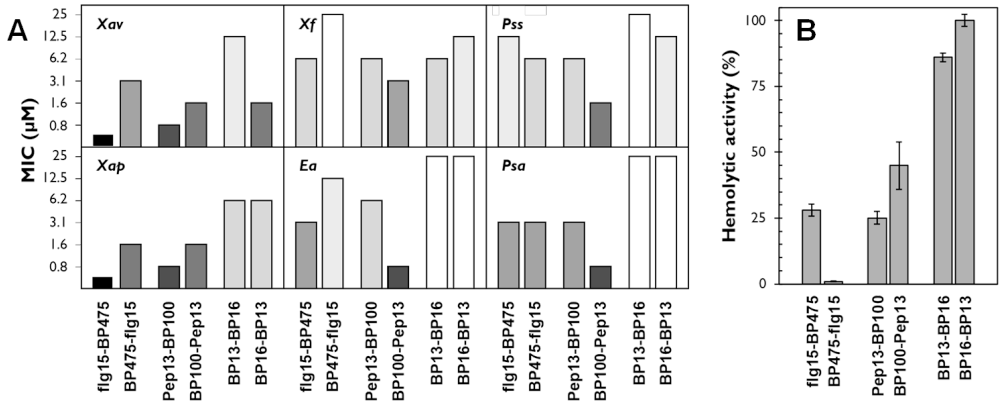

Fig. 1. A) Antibacterial activity (MIC) of selected peptide conjugates against Xanthomonas axonopodis pv. vesicatoria (Xav), Xanthomonas fragariae (Xf), Xanthomonas arboricola pv. pruni (Xap), Erwinia amylovora (Ea), Pseudomonas syringae pv. syringae (Pss) and Pseudomonas syringae pv. actinidiae (Psa). For each sequence the lowest value of the MIC range is represented. B) Hemolysis of the peptide conjugates at 150 μM, expressed as a percentage compared to melittin.

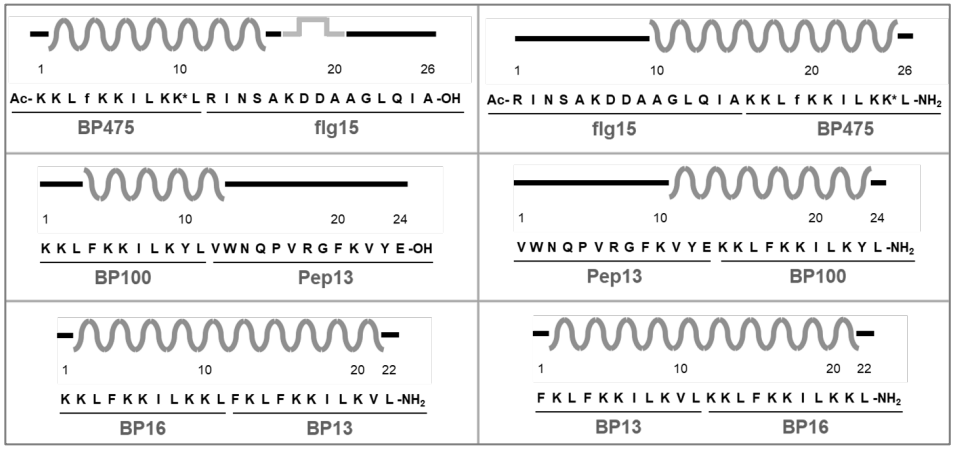

*Fig. 2. Schematic representation of the secondary structure of peptide conjugates predicted by NMR. Dark grey curves mark the α-helical region; grey lines β-turns; and black lines assign residues in a random coil. Lipopeptide **BP475** incorporates a butanoyl group at the side-chain of the lysine with an asterisk, and a D-Phe which is written in lowercase letter.*

As shown in Figure 2, in **flg15-BP475, flg15-BP475, Pep13-BP100** and **BP100-Pep13**, the most active peptide, the antimicrobial fragment (**BP475** or **BP100**) folded into an α helix, whereas the elicitor moiety (**flg15** or **Pep13**) remained unstructured as a random coil. In addition, these peptides have a low hydrophobic moment (0.12-0.33) and a positive charge of +5 or +6. In contrast, **BP13-BP16** and **BP16-BP13**, which showed the worst biological activity profile were completely structured as an α helix and have significantly higher hydrophobicity (>0.80) and charge (+10).

Furthermore, peptide conjugate **flg15-BP475** was characterized by NMR in presence of anionic SDS-d_{25} and zwitterionic DPC-d_{38} micelles to mimic biological membranes. Results showed a similar Hα chemical shift to that observed in presence of 30% CF_3CD_2OD, thus displaying a similar folding. These results point out that TFE constitutes a suitable solvent to analyze these peptide conjugates. Moreover, NMR results were in agreement with those obtained from circular dichroism (Figure 3A), suggesting that in all conditions tested, except for in water, **flg15-BP475** partially folds into an α-helix.

In order to analyze the interactions of the folded peptide **flg15-BP475** with the environment, we used Mn^{2+} as a hydrophilic paramagnetic probe, which results in the selective quenching of the solvent-

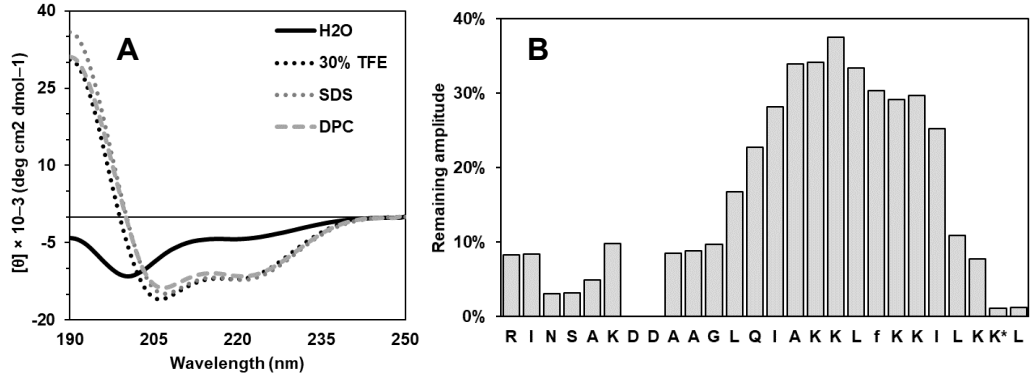

*Fig. 3. A) Circular dichroism of **flg15-BP475** B) Relative change of intensities of Hα-NH TOCSY cross peaks acquired in DPC micelles after the addition of $MnCl_2$.*

exposed residues [7]. The relative change in the intensity of the signals was quantified by determining the remaining amplitude in the Hα/NH TOCSY cross-peaks before and after the addition of $MnCl_2$ (Figure 3B). Residues Ala^{10} to Lys^{24}, that fold into an α-helix, are less exposed to the solvent and, thus, strongly interact with the micelles, showing a remaining amplitude of the cross peaks >10% after the addition of Mn^{2+}.

Overall, this study suggests the importance of a moderate amphipathic character and a positive charge around +5 for an optimal biological profile. In future works, we expect to relate all these physicochemical parameters with the mechanism of action of these peptide conjugates.

Acknowledgments

We acknowledge the Serveis Tècnics de Recerca of the University of Girona for the mass spectrometry analysis. This research was funded by MCIU/AEI/FEDER, UE, grant numbers AGL2015-69876-C2-2-R, AGL2015-69876-C2-1-R, RTI2018-099410-B-C22, and RTI2018-099410-B-C21. G.R.-L. is recipient of a fellowship from the University of Girona (IFUdG2020). P.C.-F. is recipient of a fellowship from Spain Ministerio de Ciencia, Innovación y Universidades (FPU2020).

References

1. Kumar, P., Kizhakkedathu, J.N., Straus, S.K. *Biomolecules* **8**, 1-24 (2018), http://dx.doi.org/10.3390/biom8010004
2. Badosa, E., Planas, M., Feliu, L., Montesinos, L., Bonaterra, A., Montesinos, E. *Microorganisms* **10**, 1784 (2022), http://dx.doi.org/10.3390/microorganisms10091784
3. Oliveras, À., Baró, A., Montesinos, L., Badosa, E., Montesinos, E., Feliu, L., Planas, M. *PLoS ONE* **13**, e0201571 (2018), http://dx.doi.org/10.1371/journal.pone.0201571
4. Oliveras, À., Moll, L., Riesco-Llach, G., Tolosa-Canudas, A., Gil-Caballero, S., Badosa, E., Bonaterra, A., Montesinos, E., Planas, M., Feliu, L. *Int. J. Mol. Sci.* **22**, 6631 (2021), http://dx.doi.org/10.3390/ijms22126631
5. Oliveras, À., Camó, C., Caravaca-Fuentes, P., Moll, L., Riesco-Llach, G., Gil-Caballero, S., Badosa, E., Bonaterra, A., Montesinos, E., Feliu, L., Planas, M. *Appl. Environ. Microbiol.* **88**, e0057422 (2022), http://dx.doi.org/10.1128/aem.00574-22
6. Hafsa, N.E., Arndt, D., Wishart, D.S. *Nucleic Acids Res.* **43**, 370-377 (2015), http://dx.doi.org/10.1093/nar/gkv494
7. Pandit, G., Ilyas, H., Ghosh, S., Bidkar, A.P., Mohid, S.A., Bhunia, A., Satpati, P., Chatterjee, S. *J. Med. Chem.* **61**, 7614-7629 (2018), http://dx.doi.org/10.1021/acs.jmedchem.8b00353